Short communication

Anode morphology and performance of micro-tubular solid oxide fuel cells made by aqueous electrophoretic deposition

J.S. Cherng [a,*], C.C. Wu [a], F.A. Yu [a], T.H. Yeh [b]

[a] Department of Materials Engineering, Ming Chi University of Technology, 84 Gungjuan Rd., Taishan, Taipei 24301, Taiwan
[b] Center for Thin Film Technologies and Applications, Ming Chi University of Technology, 84 Gungjuan Rd., Taishan, Taipei 24301, Taiwan

HIGHLIGHTS

▶ Consecutive aqueous EPD plus single-step co-sintering was employed to make anode-supported micro-tubular SOFC.
▶ Suspension behavior of the 8YSZ–NiO composite slurry is dominated by NiO.
▶ Deposition rate increases with current density and solid loading but decreases with surfactant concentration.
▶ Porosity decreases with increasing deposition rate.
▶ The highest power density was obtained for the anode containing 70 wt% NiO.

ARTICLE INFO

ABSTRACT

Anode-supported micro-tubular solid oxide fuel cells (SOFCs) are manufactured by aqueous electrophoretic deposition (EPD). The process of these micro-tubular SOFCs includes consecutive aqueous EPDs of a porous anode layer (8YSZ–NiO), a dense electrolyte layer (8YSZ), and a porous cathode layer (LSM) onto a thin wire electrode, followed by stripping, drying, and a single-step co-sintering. The microstructure of the micro-tubular SOFCs, including the thickness and porosity of each layer, is controlled by the processing parameters such as solid loading, current density, deposition time, and sintering temperature. In particular, the effects of the morphology of the anode layer on the electrochemical performance of such micro-tubular SOFCs are investigated and discussed based on the microstructural and voltage–current–power analyses.

1. Introduction

Solid oxide fuel cell (SOFC) outperforms other types of fuel cells in many respects, including a higher efficiency and the elimination of the need for external reforming or platinum catalyst, etc. However, its high operating temperature not only restricts the selection of useable materials but also causes such problems as slower start-up, electrode sintering, interfacial diffusion between the electrolyte and electrodes, and thermal stresses due to operation cycling. This difficulty can be solved by adopting a new class of SOFC design, so-called micro-tubular SOFC [1–9], which can benefit from both the higher efficiency of planar design and the easier packaging of tubular design, due to the increased reactive area per unit volume. However, most researchers in this field employed such manufacturing methods as extrusion and dip coating which might suffer from poor controllability and repeatability, etc.

In views of improving the manufacturing as well as of lowering the ohmic resistance and concentration polarization, we have developed [10,11] a novel method of making anode-supported micro-tubular SOFCs which employs aqueous electrophoretic deposition (EPD) to consecutively deposit the anode, electrolyte, and cathode layers on a thin Cu wire, followed by stripping, drying and a single-step co-sintering. Among the three layers of deposits, the anode layer is the most complicated in which three phases, i.e., 8YSZ (8-mol% yttria stabilized zirconia), NiO and pore, co-exist and each and every one of them affects the properties of the anode and the overall performance of the SOFC. This paper tries to address this issue by varying the composition of the anode suspension for EPD and inspecting the resultant microstructure and electrochemical properties correspondingly.

* Corresponding author. Tel.: +886 2 29089899; fax: +886 2 29084091.
E-mail address: cherng@mail.mcut.edu.tw (J.S. Cherng).

2. Experimental

NiO (NiO-F, Inco) and 8YSZ (HSY-8.0, Daiichi Kigenso) powders, according to a designed ratio, were mixed and attrition milled in distilled water. Suspensions with various solid loadings of such anode (8YSZ–Ni cermet, upon reduction at work), electrolyte (8YSZ) and cathode ($La_{0.8}Sr_{0.2}MnO_3$, LSM, Ningbo Institute of Material Technology and Engineering) ceramic powders, respectively, were made by mixing the powders with distilled water using a shear mixer and an ultrasonic sonicator. To prevent the colloids from agglomeration and sedimentation, suitable amounts of ammonium polyacrylate (PAA-NH$_4$, Darvan 821A, R.T. Vanderbilt, USA) were added as dispersant. PAA-NH$_4$ would dissociate in water so that the PAA$^-$ ions would adsorb to ceramic particles to stabilize them electrosterically. Zeta potentials of these suspensions were determined by laser Doppler velocimetry. The details of suspension preparation and evaluation, as well as the setup of constant-current EPD can be found elsewhere [12].

The EPD cell consisted of a Cu wire (150 μm in diameter) anode surrounded by a hollow cylinder Ni cathode, both immersed in one of the aforementioned suspensions. The distance between these two electrodes was 1.5 cm. EPD was conducted under a constant-current control at various current levels. The process of a micro-tubular SOFC was carried out by EPD (8YSZ–NiO) → drying → EPD (8YSZ) → drying → EPD (LSM) → drying, then followed by stripping from the Cu wire, complete drying, and co-sintering at 1250 °C for 2 h in order to obtain a final structure consisting of a porous anode layer, a dense electrolyte layer and a porous cathode layer respectively. The microstructure of the anode layer was revealed by scanning electron microscopy using back-scattered electron (BSE) image for atomic-number contrast, and each constituent was stereometrically measured by a linear intercept method. The electrical conductivity of the reduced anode, about 8 mm in length and 240 μm in thickness resulting from a 100 sec-deposition as the innermost layer of the co-sintered SOFC tube, was measured from its two ends by a multimeter. The electrochemical performance of the micro-tubular SOFC was investigated by the V–I–P (voltage–current–power) measurement.

3. Results and discussion

Fig. 1 shows the variations of zeta potential with PAA-NH$_4$ addition for 8YSZ, NiO, and two composite slurries of them with their 8YSZ:NiO (wt%) being 5:5 and 3:7 respectively. It is obvious that about 1 wt% of PAA-NH$_4$ addition is enough to stabilize the
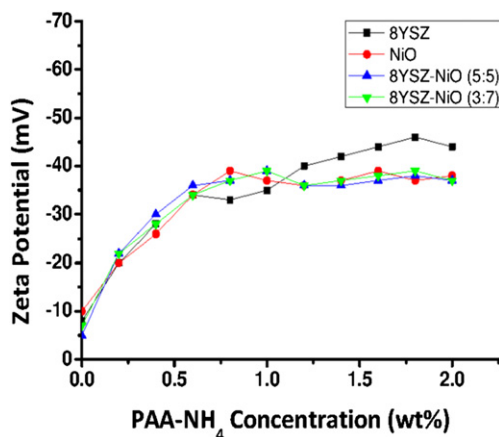
slurry, and the suspension behavior of 8YSZ–NiO composite slurry is dominated by NiO even at 50 wt% NiO, not to mention higher NiO contents.

The effects of three major EPD process variables, i.e., current density, solid loading and surfactant concentration, on the deposition rate and porosity (after sintering at 1250 °C) of 8YSZ and 8YSZ–NiO are shown in Fig. 2(a)–(c) respectively. It is observed that the deposition rate increases with current density and solid loading, but decreases with increasing PAA-NH$_4$ concentration. The current density effect is expected from either Hamaker's equation or Faraday's law [13], while a higher solid loading results in larger agglomerates, less surface area for PAA$^-$ adsorption, and thus

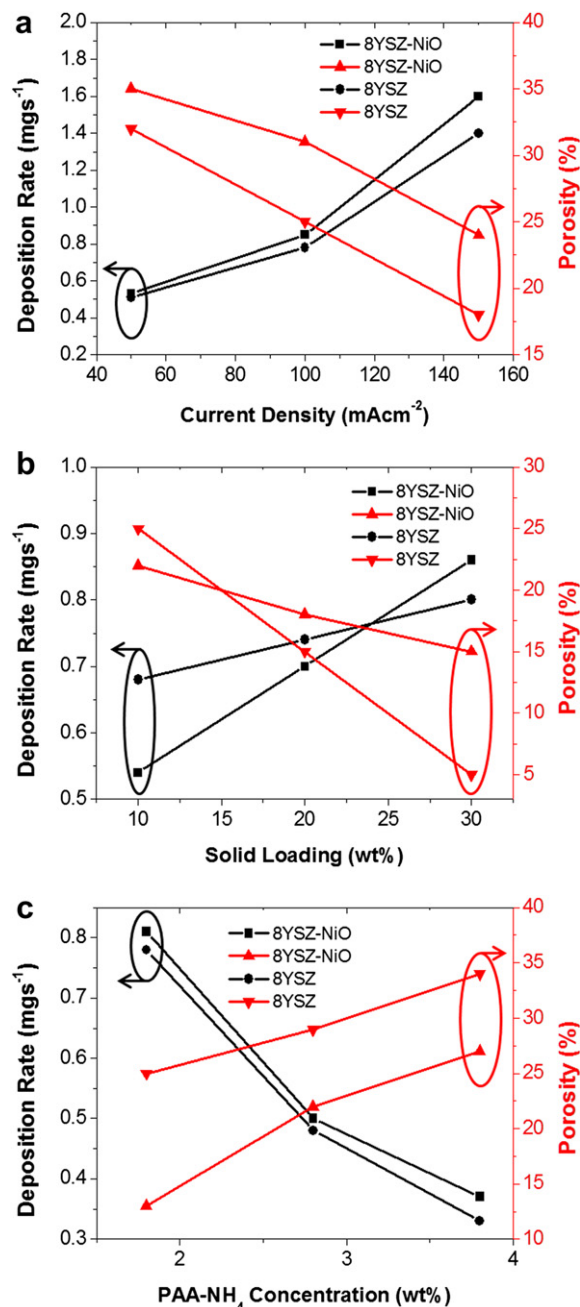**Fig. 2.** Variations of deposition rate and porosity (after sintering at 1250 °C) with (a) current density, (b) solid loading, and (c) surfactant concentration for 8YSZ and 8YSZ–NiO single layer respectively. The default deposition conditions were 100 mA cm^{-2}, 10 wt% solid loading, and 1.8 wt% PAA-NH$_4$.

Fig. 1. Variations of zeta potential with PAA-NH$_4$ concentration for YSZ, NiO and their mixtures.
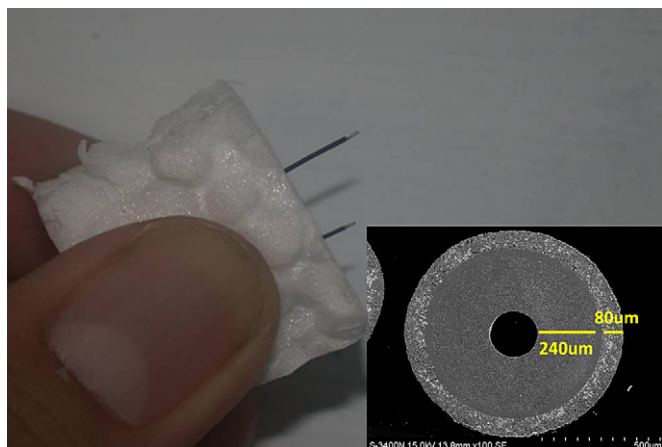
Fig. 3. A photograph (with an inset for close-up) of typical micro-tubular SOFCs made by consecutive EPD and single-step co-sintering.

a higher deposition rate under a constant-current EPD condition [13]. On the other hand, excess PAA-NH$_4$ addition causes more freely-suspended PAA$^-$ which is also electrophoretically deposited and thus decreases the deposition rate of ceramic powders. However, no matter what parameter is adjusted, the porosity always decreases with increasing deposition rate as can be observed throughout Fig. 2(a)—(c). This phenomenon implies a denser packing at a higher deposition rate, due possibly to a higher momentum of the colloid during EPD. Finally, it should be noted that the data shown in Fig. 2 are for the YSZ single layer or YSZ—NiO single layer only (the LSM single layer behaves similarly yet not shown here for clarity). When making three-layered SOFC tubes, it has been found that co-sintering tends to produce a denser YSZ layer and more porous anode/cathode layers due to differential sintering stress [10,11].

Fig. 3 shows a photograph (with an inset for close-up) demonstrating the minute size of such micro-tubular SOFCs made by consecutive EPD and co-sintering at 1250 °C. The BSE images of its 8YSZ—NiO layer (innermost) at 70, 80 and 90 wt% NiO are shown in Fig. 4(a)—(c) respectively, where the brightest phase is 8YSZ, the darker NiO, and the darkest pore, identified from their atomic-number contrast. After stereometrically measured by a linear intercept method, the effects of NiO content on the volume percent and feature size of each constituent are shown in Fig. 5(a) and (b) respectively. It is seen that the porosity remains about 30 vol% regardless of the NiO content. The 8YSZ remains around 0.6 μm, while the NiO grows from 2.2 to 2.4 μm, and the pore grows the fastest from 1.1 to 1.4 μm when the NiO content increases from 70 to 90 wt%. The corresponding electrical conductivity becomes measurable above 70 wt% NiO, and then increases with NiO content as shown in Fig. 6. The apparent threshold composition of 70 wt%
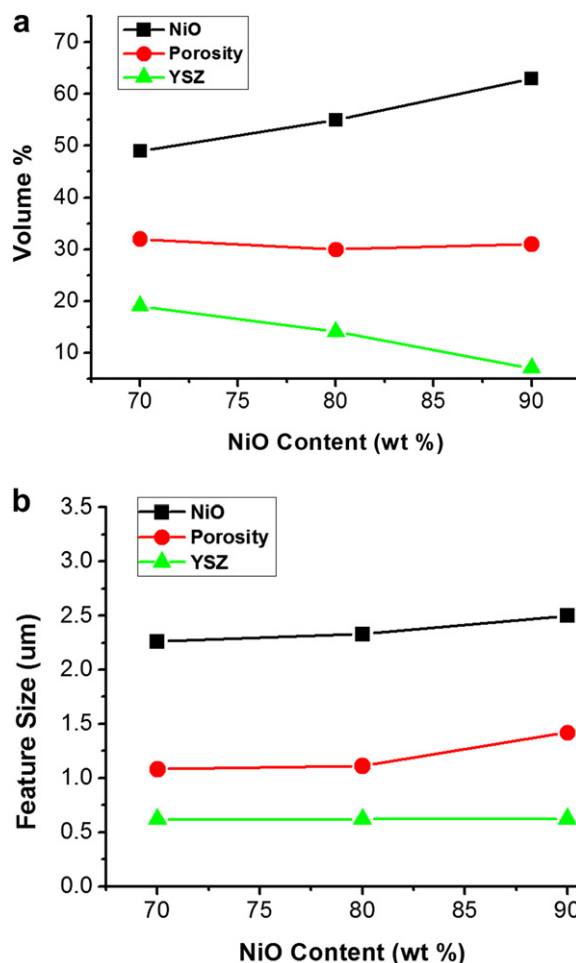

Fig. 5. Effects of NiO content on (a) volume percent, and (b) feature size of each constituent of the anodes shown in Fig. 4.

NiO for the composite slurry simply reflects the resultant minimum volume percent of NiO, i.e., ∼ 50 vol% as observed from Fig. 5(a), required for a decent electronic conductance (after being reduced into Ni).

Nevertheless, the anode (and the cathode too) needs to be a mixed ionic-electronic conductor (MIEC) so that the SOFC can function properly. The electrochemical performances of such micro-tubular SOFCs can be seen in Fig. 7 where the V—I—P analysis was carried out at 800 °C, for the three types of anodes shown in Fig. 4, with a 50 sccm fuel of 20% H$_2$ in N$_2$ flowing inside the tube and air outside. The open circuit voltages (V_{oc}) all appear to be larger than 1.2 V, i.e., close to the theoretical value estimated from the Nernst equation, verifying the gas-tightness of the 8YSZ
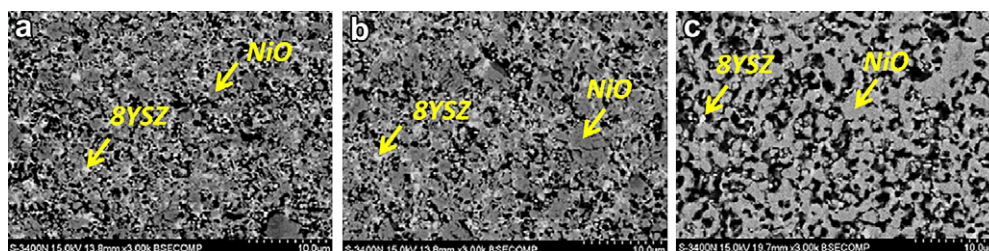

Fig. 4. Back-scattered electron images of the 8YSZ—NiO layer (innermost layer of the micro-tubular SOFC) at (a) 70, (b) 80 and (c) 90 wt% NiO. The EPD was performed at 100 mA cm^{-2}, 30 wt% solid loading, and 3.8 wt% PAA-NH$_4$.
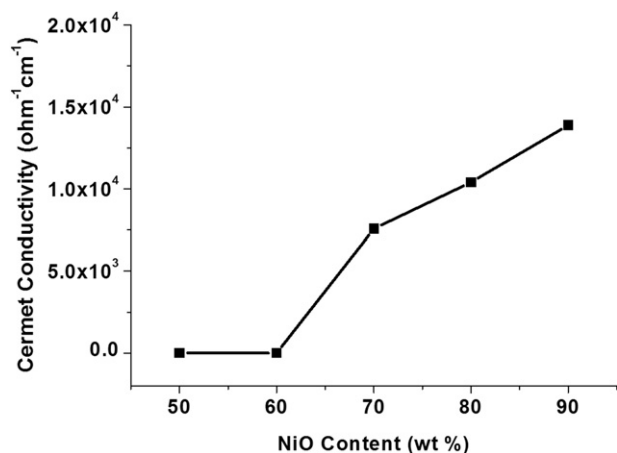
Fig. 6. Variation of the electronic conductivity of the anode layers shown in Fig. 4 (after reduction) with NiO content.
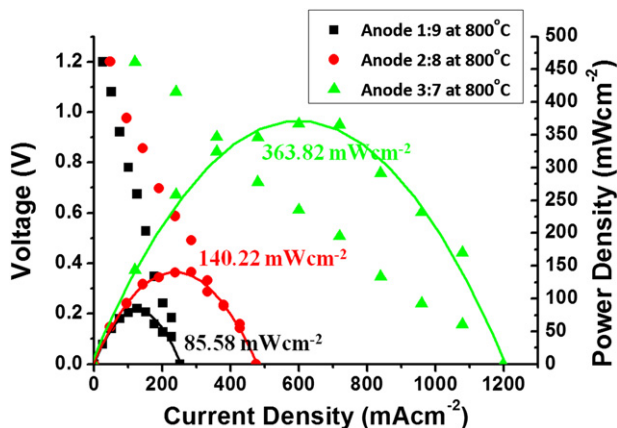

Fig. 7. Electrochemical performances of such micro-tubular SOFCs with various anode compositions. The V–I–P analysis was carried out at 800 °C with a 50 sccm fuel of 20% H_2 in N_2 flowing inside the tube and air outside.

electrolyte layer. The optimum power density at 800 °C reaches 363.8 mW cm^{-2} for the anode with 70 wt% NiO, and degrades to lower values at higher NiO contents. This observation confirms the aforementioned requirement for the anode being a decent MIEC. Higher NiO contents, say, >80 wt%, lack of enough 8YSZ phase for the ionic conduction despite a better electronic one. Thus the best anode composition in this study remains to be 70 wt% NiO, where

the optimal compromise between ionic and electronic conductions rests. Lastly, it should be mentioned that there are clearly much more room to further improve the power density, say, by using a thinner 8YSZ electrolyte layer and purer fuel gas, as well as by optimizing the porosities/thicknesses of the anode/cathode layers, etc. A preliminary modification of the layer thicknesses, from 240-35-80 μm to 180-15-80 μm for anode–electrolyte–cathode, raised the power density to a value of 491.8 mW cm^{-2} already.

4. Conclusions

Consecutive aqueous EPD plus single-step co-sintering have been successfully employed to make anode-supported micro-tubular SOFCs using 8YSZ–Ni, 8YSZ and LSM as the anode, electrolyte and cathode material respectively. The suspension behavior of the 8YSZ–NiO composite slurry is dominated by NiO. The deposition rate increases with current density and solid loading but decreases with surfactant concentration, while the porosity decreases with increasing deposition rate. The highest power density reaches 363.8 mW cm^{-2} at 800 °C when the anode contains 70 wt% NiO and behaves as a decent MIEC.

References

[1] N.M. Sammes, Y. Du, R. Bove, J. Power Sources 145 (2005) 428–434.
[2] S.B. Lee, T.H. Lim, R.H. Song, D.R. Shin, S.K. Dong, Int. J. Hydrogen Energy 33 (2008) 2330–2336.
[3] S.B. Lee, T.H. Lim, R.H. Song, D.R. Shin, S.K. Dong, Int. J. Hydrogen Energy 35 (2010) 8654–8662.
[4] R. Campana, R.I. Merino, A. Larrea, I. Villarreal, V.M. Orera, J. Power Sources 192 (2009) 120–125.
[5] H. Luebbe, J.V. Herle, H. Hofmann, P. Bowen, U. Aschauer, A. Schuler, F. Snijkers, H. Schindler, U. Vogt, V. Lalanne, Solid State Ionics 180 (2009) 805–811.
[6] T. Suzuki, T. Yamaguchi, Y. Fujishiro, M. Awano, J. Power Sources 160 (2006) 73–77.
[7] T. Suzuki, Y. Funahashi, T. Yamaguchi, Y. Fujishiro, M. Awano, J. Power Sources 171 (2007) 92–95.
[8] T. Suzuki, T. Yamaguchi, Y. Fujishiro, M. Awano, J. Power Sources 163 (2007) 737–742.
[9] T. Suzuki, Y. Fujishiro, T. Yamaguchi, Y. Fujishiro, M. Awano, J. Alloys Compd. 451 (2008) 632–635.
[10] J.S. Cherng, M.Y. Ho, T.H. Yeh, W.H. Chen, Ceram. Int. 38S (2012) S477–S480.
[11] J.S. Cherng, C.C. Wu, W.H. Chen, T.H. Yeh, Ceram. Int. 2012. http://dx.doi.org/10.1016/j.ceramint.2012.10.144.
[12] J.S. Cherng, J.R. Sau, C.C. Chung, J. Solid State Electrochem. 12 (2008) 925–933.
[13] C.C. Chung, M.S. thesis, National Dong Hwa Uviversity, Taiwan, 2002.